JOURNAL OF THE PHYSICAL SOCIETY OF JAPAN Vol. 13, No. 12, DECEMBER, 1958

On the Ferromagnetic Phase in Manganese-Aluminum System

By Hiroshi KŌNO

The Research Institute for Iron, Steel and Other Metals, Tōhoku University, Sendai

(Received August 15, 1958)

A metallographical investigation of manganess-aluminum system was made in the compositional range of 47% to 60% of manganese, with the results of a new hexagonal close-packed phase and a metastable tetragonal ferromagnetic phase derived therefrom. The conditions necessary for formation, structure, stability and thermal and magnetic properties of the latter phase have been studied. A discussion was also given on its magnetic properties.

§ 1. Introduction

The existence of a ferromagnetic phase in manganese-aluminum system was pointed out by Hindricks[1] in 1908; Ishiwara[2] and later Köster[3] et al. made further metallographical investigations on the nature of this phase, but they failed to find its well-defined positions in the phase diagram of this binary system. Also the structure and thermal and magnetic properties of this phase have not yet been studied in detail. Moreover, there are some inconsistencies between the reported those diagrams and magnetic properties found by these authors: According to Ishiwara's phase diagram, the composition corresponding to the maximum magnetization in the ferromagnetic range lies in the two-phase region of α and δ. For the purpose of clarifying the metallographical nature of this phase, the present writer studied this system with specimens in the compositional range from 47% to 60% Mn, and with various heat treatments; basing on the results obtained, the phase diagram of this region was studied. Then the stability, the structure and thermal, magnetic and electrical properties of the ferromagnetic phase were then investigated.

§ 2. Specimens and Experimental Method

Electrolytic manganese (purity 99.9%) and aluminum pieces (99.99%) were put together in Tammann tubes in desired proportions, the inside of which was coated with alumina, and melted in an induction furnace in air; in this way mother alloys of 40 and 70 atomic per cent manganese at charge were prepared. (Chemical analysis gave 40.9% and 72.5% Mn respectively.) They were crushed, mixed in proper proportions and melted in the same way as mentioned above and cast into bars 5 mm in diameter. The specimens thus obtained were named A_{47}, A_{48}, etc., the suffices indicating the atomic percentage of charged manganese content. During the course of melting the actual composition may be changed slightly from the initially charged one, but the shift of composition on the whole, is considered to occur regularly, so that no serious error may be introduced into a description of their physical properties in terms of charged compositions. For reference, the result of chemical analysis is given in Table I.

Table I. Chemical analysis of the specimens.

	A_{49}	A_{50}	A_{51}	A_{53}	A_{54}	A_{56}	A_{58}	A_{60}
Atomic per cent of manganese	49.1	50.1	52.2	53.8	55.1	57.1	57.9	62.5

The magnetic measurement was carried out by a ballistic method or with a magnetic balance described elsewhere[4], the X-ray structure analysis by the Debye-Scherrer method with Fe–K_α radiation and the thermal analysis by an adiabatic method, the detailed description of which was given by Nagasaki[5] and Takagi as well as Maeda[6]. This method is considered to be good for the magnitude estimation of the latent heat for the first order transformations. For the purpose of keeping adiabatic condition at high temperatures in the present experiment, a specimen container of nickel, 5 mm in thickness, was used, and the container was further shielded by a hollow steel cylinder of 1 mm in thickness. In this way the temperature distribution in the nickel-container was homogenized. Moreover, in the present case a specimen vessel of nickel was

used, which was filled by the bar-formed specimens of proper length.

§ 3. Results of Metallographical Study

First the results of metallographical study will be described. Since the existence of a eutectoid reaction was expected above 800°C in the compositional range mentioned above, the specimens were subjected to an annealing for 1 hour at 950°C to remove the segregation, then slowly cooled to 700°C, annealed again for about 5 hours at this temperature and then cooled slowly down to room temperature in vacuum. From the fact that the specific heat *vs* temperature curves of the specimens annealed for 30 minutes and those for 3~4 hours at 700°C did not differ from each other, it may be considered that the equilibrium at 700°C has almost been reached by the heat treatment mentioned above.

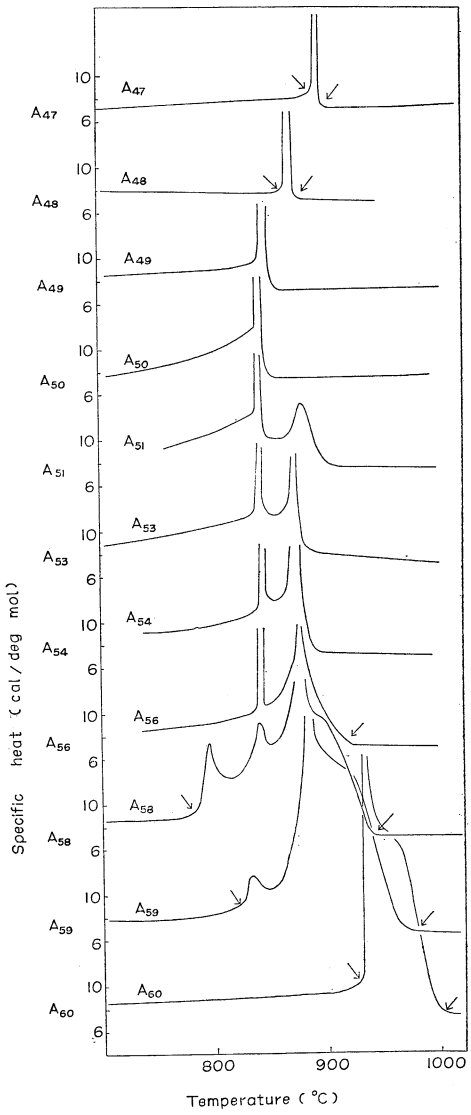

Fig. 1. Specific heat *vs* temperature curves

First of all the specific heats of these specimens were measured at the heating rate of about 2 deg./min. As shown in Fig. 1, the absorptions of heat with the latent heat type could be observed both at the temperatures 840°C and 870°C. Such measurements were repeated several times and it was found that the result here mentioned was quite reproducible. Moreover, it must be noted that the absorbed heat quantities as well as the temperatures of the heat absorption were hardly affected by the lowering of the heating rate to a value one-third of the above mentioned one during the measurement. From the results of the specific heat measurements, each absorbed heat quantity at 840°C was plotted against the composition from A_{49} to A_{57} in

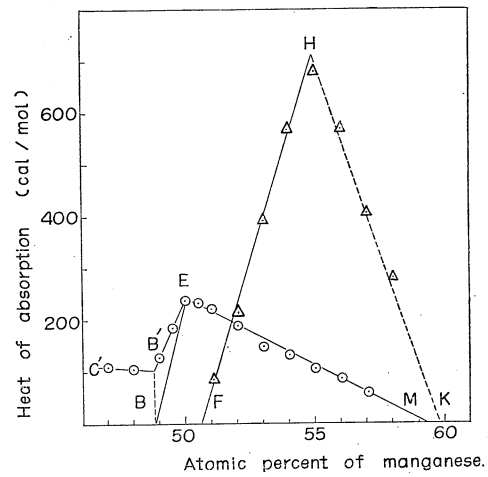

Fig. 2. Heat of absorption at 840°C, 870°C and $\zeta \rightarrow \zeta'$ reaction. For the points ○ and △, the accuracy of the measurement is not sufficient.

Fig. 2; As can be seen from the result in Fig. 2, the absorbed heat quantity of the latent heat type is greatest at 50% and decreases linearly with the change of composition on both sides. Thus the triangle $B'EM$ was obtained. Moreover, the absorbed heat quantity for peaks A_{47} and A_{48} were also plotted, and a line $B'C'$ was obtained. Based on these results as well as on the results of X-ray analysis described in the next paragraph, it is to be proposed that the latent heat ob-

served at 840°C is due to a eutectoid reaction. The eutectoid product was named ζ'-phase. However, it is to be considered here that the two phase region $\zeta'+\zeta$, ζ being one of the reactants of the eutectoid reaction, is very narrow, so the mutual mixing of ζ and ζ', which follows the eutectoid reaction, takes place at very narrow temperature range, and the heats of both reactions cannot be separated by the present specific heat measurement. Hence, it follows that heat quantities plotted in the compositional range between B and E in Fig. 2 represent the total evolved heats due to these two reactions. In this case the bracking point B' is the end point of the eutectoid line. Consequently the line EB represents the heat of the eutectoid reaction in the compositional range from B to E, and the range in which the eutectoid reaction occurs

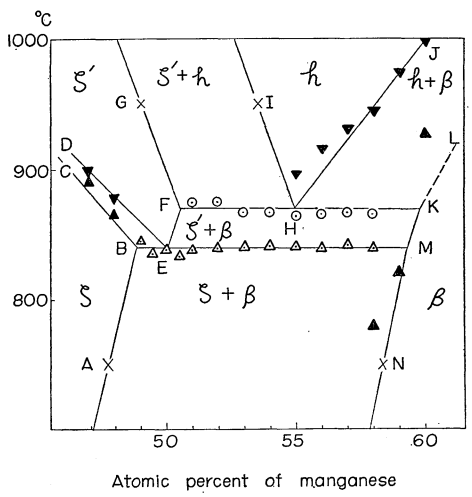

Fig. 3. Phase diagram in the vicinity of MnAl. The upright and inverted black triangles ▲ and ▼ in this figure correspond to the temperatures of appearance and disappearance of excess specific heat respectively. These points are shown by signs ↘ and ↙ in Fig. 1.

extends from point B of about 49% Mn to point M of about 59.5%, and the composition of the eutectoid point E is 50% Mn. The temperatures at which such heat absorption occurs are indicated by △ for various compositions in Fig. 3 and thus the eutectoid line BEM is obtained.

Now another supplementary fact for the above mentioned reasoning can be seen from Fig. 1 at temperatures just below 840°C. Specific heats per mol*. C_p of the alloy A_{47}, A_{48} and A_{60} do not differ so remarkably from the value expected from the Dulong-Petit law, while those of the other specimens, the compositions of which lie in the range of the eutectoid line, show excess specific heat over the Dulong-Petit value, which is supposed to be due to the solubility change of both phases in the two-phase region $\zeta+\beta$ under BEM line in Fig. 3. It may be confirmed from such behaviors of the specific heats of the alloys that the two-phase region extends over the compositional range from about 49% Mn to about 59% Mn at temperatures just below 840°C. The peaks of A_{47} and A_{48} correspond to the heat absorption which is caused by the intersection of the two-phase region $\zeta+\zeta'$ (see Fig. 3).

Now, the absorbed heat quantities at 870°C are also plotted against composition in Fig 2. As can be seen from this figure, the quantity of the latent heat absorbed at 870°C is greatest at 55% Mn and decreases linearly with change of composition on both sides of the maximum point, as is shown in Fig. 2. As can be seen from Fig. 1, the excess specific heat over the Dulong-Petit value is also seen in the specimens from A_{51} to A_{59} between 840°C and 870°C, and corresponds to the solubility change of both phases in the two phase region $\zeta'+\beta$. Based on these results, it may be supposed that the latent heat observed at 870°C is due to another eutectoid reaction. As can be estimated from Fig. 2, the range in which the eutectoid reaction mentioned here occurs extends from point F at about 50.5% Mn to point K at abont 60% Mn in Fig. 3, and the eutectoid point H lies at 50% Mn. The temperatures at which such heat absorption occurs are also indicated against composition by ⊙ in Fig. 3 and thus the eutectoid line FHK is obtained in the same was as in the case of the line BEM. The eutectoid product is named h-phase. The excess specific heat of the specimens from A_{55} to A_{60} above 870°C will be due to the solubility change of the both phases in the two-phase region $h+\beta$. The excess specific heat observed over the Dulong-Petit value in A_{51}, A_{52} and A_{53} was relatively small, which can be accounted for by assuming that

* Mol number in this case was calculated by the expression $54.93x+26.98\{(100-x)/100\}x$ being the atomic percent of manganese.

the phase boundaries between the two-phase region $\zeta'+h$ and the single phase region ζ'- or h-phase are nearly perpendicular to the composition axis. Based on these results as well as on the results of X-ray analysis described in the following paragraph, the eutectoid reaction at 870°C was confirmed.

There are peaks in the neighbourhood of 790°C, 830°C and 930°C on the specific heat v.s. temperature curves of A_{58}, A_{59} and A_{60} respectively. The values of C_p on the lower temperature side than these peaks are somewhat larger than those expected from the Dulong-Petit law, but as will be described later, X-ray analysis suggests that these specimens are in the single phase region β. From these facts, these peaks may be accounted for by assuming that the superheated β-phase suddenly decomposes into β- and ζ- or h-phases, and the specific heat v.s. temperature curves show the transformation of latent heat type.

The results of the X-ray analysis will now be described. All the specimens were annealed at 950°C for 20 minutes or at 750°C for 1 hour and then quenched into water, smashed into powder, and the Debye photographs were taken. No significant differences was found between diffraction patterns of the specimens quenched from 950°C in ζ'region and those from 750°C in ζ-region. It was difficult to make structure analysis from the diffraction lines of these two phases.

Observed intensities and Bragg angles of the Debye-Scherrer lines of quenched specimen A_{54} from the region of h-phase are shown in Table II. As the table shows all the lines can be indexed, by assuming a hexagonal close-packed form. ($c/a=1.63$, $c=4.38$Å, $a=2.69$Å) The β-phase is of the β–Mn type structure[7].

Table II. X-ray analysis of h-phase (quenched state).

Observed $\sin\theta$	Observed line intensity (Fe-K_α)	Line inde	Calculated $\sin\theta$ with the lattice parameters $a=2.69$Å $c=4.38$Å
0.416	s.	$(10\bar{1}0)$	0.416
0.445	s.	(0002)	0.445
0.472	v.s.	$(10\bar{1}1)$	0.471
0.608	m.	$(10\bar{1}2)$	0.609
0.720	m.	$(11\bar{2}0)$	0.720
0.786	m.	$(10\bar{1}3)$	0.786
0.846	m.	$(11\bar{2}2)$	0.846
0.858	f.	$(20\bar{2}1)$	0.861
0.886	m.	(0004)	0.889

v: very, f: faint, m: medium, s: strong.

To determine phase boundaries, the Bragg angles θ of some strong lines of the Debye-Scherrer photographs taken with Fe–K_α radiation were plotted against composition. The phase boundaries were determined from the breaking points of the Bragg angle v.s. composition curve, the angle being independent of composition in the two phase region. The points N, A, G and I in Fig. 3 were obtained by this method.

From X-ray analysis of the specimens quenched from 750°C it was confirmed that Al-rich ζ-phase and M-rich β-phase coexist at 750°C in the compositional range from about 48 to 58% Mn, and the phase boundary line MN was determined by connecting M and N determined as mentions above, and the line AB was determined in the same way. The phase boundary line HJ was also determined from H and points ▼ of A_{55}, A_{56}, $\cdots$, A_{60} the CB line from point B and points ▲ of A_{47}, A_{48}, and the DE line from point E and points ▼ of A_{47}, A_{48}. The lines FG and HI were determined by connecting F and G, and H and I respectively, but the location of G and I from which the lattice parameters of ζ'-phase and h-phase respectively begin to change was rather poor in accuracy. The line KL could not be determined accurately, and the determination of its correct position will be a future problem.

§ 4. Physical Properties of the Ferromagnetic Phase and its Relation to Phase Diagram

From the magnetic measurements, both ζ- and β-phase as well as the quenched phase h were found to be non-ferromagnetic at room temperature, while the bar-formed specimens e.g. A_{54}, of the Al-rich side of h-phase which were cooled in air from 950°C were found to show ferromagnetism. The cooling rate was found to have some influence of the magnetic properties of the products. For an example, the cooling curves of A_{54} from 950°C are shown in Fig. 4 together with the room temperature values of the magnetization at $H_{\text{eff}}=1500$ Oe. From this figure the heat evolution due to the transformation h-phase → ferromag-

netic phase can be observed at about 750°C. Therefore, the rate of cooling shown by B or C for A_{54} in Fig. 4 is considered to be appropriate for hindering the decomposition of the specimen into β- and ζ-phase and permitting the formation of the ferromagnetic phase. It was also found that the magnetization of the air-cooled specimens from 950°C increases linearly with composition in the range from 50.5% to 54% Mn. In this compositional range, the relative line intensities of ζ'- and the ferromagnetic phase varied monotonously with composition, which was seen from the X-ray analysis of the air-cooled specimens.

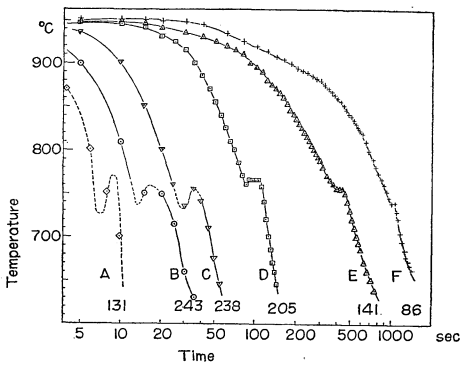

Fig. 4. Cooling curves of A_{54} measured from 950°C. The curves for air cooling are shown by B or C. The figures under the curves are the magnetization in gauss at room temperature. (H_{eff}=1,500 Oe.)

The observed Bragg angles θ and intensities of the diffraction lines in the Debye-Scherrer photograph of the ferromagnetic A_{54} specimen are shown in Table III. As shown in this table, all lines could be indexed by assuming the lattice to be tetragonal. (see the 3rd column. c/a=0.908, a=3.94Å, c=3.58) Moreover, no diffraction lines due to the β or ζ-phase were not be able to be found in the same photograph, while in the case of the Al-rich specimens the diffraction lines due to ζ'-phase were contained besides the original lines of the ferromagnetic phase and the intensity of the former increased with decreasing manganese content, while that of the latter decreases, disappearing at the composition of 50% Mn. In the Mn-rich case those due to the β-phase appeared. Hence, it is to be concluded that the specimen that could be regarded as a single phase was only A_{54} and the others contained β and ζ'-phase. Moreover, the line intensities are calculated* by assuming the CuAu type superstructure, in which Mn and Al atoms occupy alternately successive layers perpendicular to the c-axis. In this case, the manganese content is a little richer than that of aluminum, so that some of Al-atoms are substituted by excess Mn-atoms. The results of calculation are shown in Table III. In this case it can easily be

Table III. X-ray analysis of the ferromagnetic A_{54}.

Observed (Fe-K_α) sin θ	Observed line intensity	Line index	Calculated sin θ with a=3.94Å c=3.58Å	Calculated line intensity
0.271	v.f.	001	0.271	14
0.347	v.f.	110	0.348	15
0.442	v.v.s.	111	0.441	249
0.492	s.	200	0.492	92
0.540	f.	002	0.542	36
0.562	v.v.f.	201	0.562	7.3
		112	0.644	5.2
0.695	m.	220	0.696	42.5
0.731	s.	202	0.732	81.4
		221	0.746	4.3
		310	0.778	4.7
		003	0.813	1.2
0.824	v.s.	131	0.824	171
0.882 } diffuse		222	0.882	102 } 210
0.882 }	v.s.	113	0.884	105 }

v: very, f: faint, m: medium, s: strong.

shown that the structure factors of the reflections, for which the sum of h and k in the Miller index (h, k, l) is odd, vanish. As the table shows, the observed relative line intensity is seen to be consistent with the result of calculation. Hence, it is probable that the structure of the forromagnetic phase is of the superstructure of CuAu type.

Now for the purpose of testing the stability of the ferromagnetic A_{54} the variation of the magnetization of the specimens due to annealing was studied in the field of H_{eff}=1750 Oe. It was found that the intensity of the magnetization was reduced to one half of its ori-

* In the calculation, the absorption due to the specimen and the decrease of the atomic scattering factor of Mn atoms due to the K-absorption edge were taken into consideration[8].

ginal value after annealing for ten hours at 910°C and almost disappeared after 50-hours annealing. At 650°C, it decreased to one half in one hour and disappeared after 7 hours, while at 700°C it decreased to one-half in a few minutes and disappeared after 30 minutes. By 500°C annealing, however, the magnetization was found to remain constant even after 162 hours.

The specific heat of the ferromagnetic A_{54} specimen prepared by air cooling from 950°C was measured in the temperature range from 100°C to 500°C at the heating rate of about 1.5 deg/min. and then this specimen was slowly cooled to room temperature in the apparatus. The measurement was repeated quite in the same way. As can be seen from Fig. 5, curve I, which was obtained in the first run, shows a broad minimum in the neighbourhood of 300°C, while curve II, corresponding to the second run, does not show such a minimum.

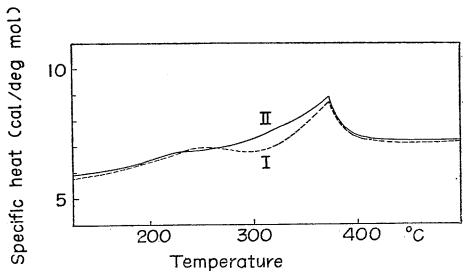

Fig. 5. Specific heat *vs.* temperature curves of the ferromagnetic A_{54}.

Measurements in subsequent runs reproduced exactly the result of the second run. However, for the specimen which was annealed for 18 hours at 400°C, the specific heat v.s. temperature curves did not show such a minimum and the results were quite reproducible within error of experiment at temperatures below 500°C. Therefore, the ferromagnetic A_{54} subjected to the low temperature annealing can be regarded as a stable phase with the superstructure of CuAu type in this temperature range, so we performed such a heat treatment for all of the specimens hereafter. From the thermomagnetic curve shown later, the peak at 373°C in Fig. 5 may be considered to be due to the magnetic transformation. When the measurement of the specific heat of the ferromagnetic A_{54} was extended to higher temperatures, a significant minimum of the specific heat appeared at about 700°C. It is considered to be due to the decomposition of the ferromagnetic A_{54} into ζ- and β-phases, the accompanying evolution producing the minimum mentioned above.

The magnetization curve for powdered ferromagnetic A_{54} was taken by the ballistic method. The H^{-2} plot of specific magnetization σ is given in Fig. 6. Thus, the extraporated saturation values at the room temperature and the boiling point of liquid nitrogen are found to be $\sigma_\infty=95.4$ and 99.6 respectively. Based on these two values, the extraporated saturation value at absolute zero $\sigma_\infty(O)$ by the formula $\sigma_\infty(T)=\sigma_\infty(O)\ (1-aT^2)$ was found to be $\sigma_\infty(O)=100$. The thermomagnetic curve at $H_{ex.}=4500$ Oe. and the sus-

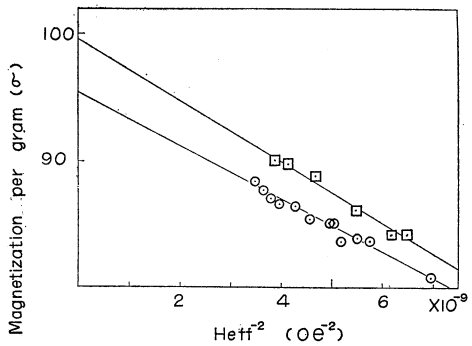

Fig. 6. The extraporated saturation values at the room temperature (⊙) and the boiling point of liquid nitrogen (⊡).

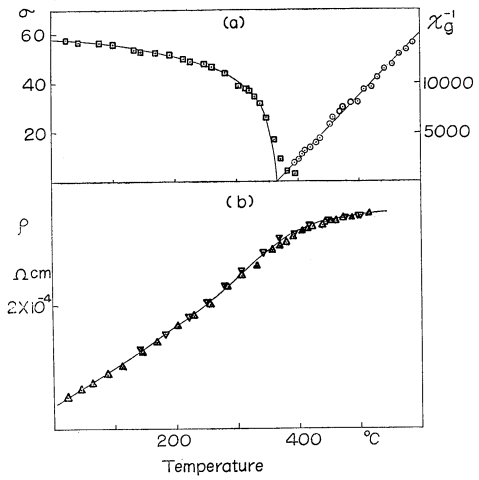

Fig. 7. Magnetization and electric resistance of the ferromagnetic A_{54}.

- ⊡ magnetization per gram (H_{ex} =4500 Oe.)
- ⊙ inverse of susceptibility per gram
- △ specific resistance } heating
- △ specific resistance ..... cooling

ceptibilities above the Curie temperature are shown in Fig. 7(a). In the ferromagnetic region the magnetization decreases with rising temperature, following a Weiss type curve, and disappears at the Curie point of about 370°C. On the heating curve of the susceptibility measurement, the Curie-Weiss law is seen to hold below 550°C, while at higher temperatures susceptibility decrease rapidly due to decomposition. The high temperature phase h shows weak paramagnetism in its stable range. It was seen from the cooling curve at the rate of about 3 deg/min. that h-phase remained unchanged until about 800°C and then decomposed. From these results, it is considered that the formation of the ferromagnetic phase is influenced by the cooling rate at about 800°C. The variation of specific resistance with temperature is shown in Fig. 7(b). The curve in the figure show a behavior usually observed in ordinary ferromagnetic metals below the Curie point.

§ 5. Discussions of the Magnetic Properties of the Ferromagnetic Phase

As stated above, the ferromagnetic phase discussed in the present investigation is supposed to be of the superstructure of CuAu type, which has a layer structure: Each (011) net plane contains mainly Mn or Al atoms respectively, stacking alternately in [001] direction of the crystal. Now we shall make a brief remark on the interatomic distance between two Mn atoms in the nearest neighbouring pair in a layer or in two adjacent layers. There are a few Mn atoms in an Al layer. The nearest neighbouring pair of Mn atoms in two adjacent layers has the distance 2.66Å, while that in a Mn layer has the distance 2.79Å. Now, according to the Bethe-Slater curve representing the relation between the exchange energy of magnetization and the interatomic distance, the exchange coupling between 3d-electrons of adjacent Mn atoms changes from antiferromagnetic to ferromagnetic at the interatomic distance of about 2.57Å. The distances between Mn atoms in our crystal are greater than this critical value, and so the occurrance of ferromagnetism in this alloy is compatible with this prediction.

The Curie temperature T_c, the absolute saturation value $\sigma_\infty(O)$, the heat of absorption per gram atom of manganese in the alloy, ΔE due to the magnetic transformation, the spin S_χ estimated from the $1/\chi$ v.s. T curve above the Curie point and the spin S_σ estimated from the saturation magnetization at $T=0$ are summarized in Table IV; these figures are obtained by assuming that all the Mn atoms are equivalent. Moreover, though not shown in Table IV, both T_c and ΔE increase with Mn content; there is an evidence that the Curie point increases by 14°C with the increase of manganese content from 54 to 55%.

Table IV.

T_c	$\sigma_\infty(0)$	ΔE	S_χ	S_σ
373°C	100	320 cal	1.16	0.70

The discrepancy between the magneton number estimated from the magnetic saturation at low temperatures and that from the Curie-Weiss representation of the susceptibilities above the Curie point may be caused partly by the difficulty in saturating the magnetization, but since the latter magneton number is significantly greater than the former, there must be another reason for this, probably related to some intrinsic nature of this material. Since the $1/\chi$ v.s. T curve follows the Curie-Weiss law, we have no strong reason to consider the material to be ferrimagnetic*.

§ 6. Summary

The ferromagnetic phase in the manganese-aluminum system was investigated together with the related phase diagram. It was found that the ferromagnetic phase is formed by cooling down the h-phase (hexagonal lose-packed form) with about 54 atomic percent of manganese at charge to the room temperature at the cooling rate of about 10 deg./sec at 800°C. The ferromagnetic phase is metastable and has the CuAu type superstructure; the shortest distance between a pair of manganese atoms within the lattice is 2.66Å. The Curie point of this phase is about 380°C, and

* One may consider that the magnetization of this substance is smaller than that predicted from the total spin alignment because of the effective smallness of the exchange energy as is often considered in the theory of collective electron ferromagnetism.

values of the mean magnetic moment per manganese atom estimated from the low temperature saturation magnetization and the Curie-Weiss representation of the susceptibilities are 1.40 and 2.31 μ_B respectively.

Acknowledgements

The present writer would like to express his sincere thanks to Profs. T. Hirone, H. Watanabe, S. Nagasaki and S. Maeda for their kind guidance during his studies of the present project in the Graduate Course of the Faculty of Science, Tōhoku University.

References

1) G. Hindricks: Z. Anorg. Chem. **59** (1908) 444.
2) T. Ishiwara: Kinzoku no Kenkyu **3** (1926) 13 (in Japanese).
3) W. Koster and W. Beckthold: Z. Metallk. **30** (1938) 294.
4) T. Hirone, S. Maeda and N. Tsuya: Rev. Sci. Instr. **25** (1954) 516.
5) S. Nagasaki and Y. Takagi: J. Appl. Phys. Japan (in Japanese) **17** (1948) 104.
6) S. Maeda: Sci. Rep. RITU. **A9** (1957) 347.
7) A. J. Bradley and P. Jones: Phil. Mag. **12** (1931) 1137.
8) A. J. Bradley and J. W. Rodgers: Proc. Roy. Soc. London **A144** (1936) 340.